Weather and Climate Extremes 4 (2014) 22–34

Contents lists available at ScienceDirect

Weather and Climate Extremes

journal homepage: www.elsevier.com/locate/wace

Forecasting the heavy rainfall during Himalayan flooding—June 2013

Anumeha Dube*, Raghavendra Ashrit, Amit Ashish, Kuldeep Sharma, G.R. Iyengar, E.N. Rajagopal, Swati Basu

National Centre for Medium Range Weather Forecasting (NCMRWF), Earth System Science Organisation (ESSO), Ministry of Earth Sciences, A-50, Industrial Area, Phase-II, Sector 62, Noida, Uttar Pradesh 201309, India

ARTICLE INFO

Article history:
Received 16 September 2013
Received in revised form
18 March 2014
Accepted 21 March 2014
Available online 8 April 2014

Keywords:
Southwest monsoon
Uttarakhand
Global Forecast System
Unified Model
Contiguous rainfall area
Event verification

ABSTRACT

On 17th June 2013 the state of Uttarakhand in India (Latitude 28.72°N to 31.45°N and Longitude 77.57°E–81.03°E) received more than 340 mm of rainfall, which is 375% more than the daily normal (65.9 mm) rainfall during monsoon. This caused heavy floods in Uttarakhand as well as unprecedented damage to life and property. In this study we aim at assessing the performance of two deterministic forecast models, Global Forecast System (GFS/T574) and Unified Model (NCUM), run at NCMRWF, in predicting the heavy rainfall observed over Uttarakhand region of India during 17–18th June, 2013.

Verification of the synoptic features in forecasts of the two models suggests that NCUM accurately captures the circulation features as compared to T574. Further verification of this event is carried out based on the contiguous rain area (CRA) technique. CRA verification is used in computing the total mean square error (MSE) which is based on displacement, volume and pattern errors. This verification technique also, confirms the better skill of NCUM over T574 in terms of forecast peak rainfall amounts, volume and average rain rate, lower MSE and root mean square error (RMSE) as well as having higher hit rates and lower misses and false alarm rates for different rainfall thresholds from Day 1 to Day 5 forecasts.

1. Introduction

Over the Indian subcontinent, the amount of rainfall received during the southwest monsoon season (June–September) is very crucial for the agriculture and in turn for the economy. In the past couple of years, there have been several cases of heavy rainfall (3–12 cm/day) events over India. The most recent events (June 2013) are the heavy rainfall observed in Maharashtra (approximately 300% more than the average during 1st to 16th June, 2013 in Mumbai and adjoining areas) and Uttarakhand (approximately 800% more than the average during 13th–19th June, 2013 in Kedarnath and adjoining areas) states of India. These led to a massive destruction of property and loss of life (more than 1000 deaths, several missing persons and more than 61,000 stranded in Uttarakhand, (Disaster Update, 18-June, 2013; Disaster Update, 19-June, 2013; Southwest monsoon-June, 2013; Southwest monsoon-July, 2013). Thus, issuing a reliable short to medium range (3–7 days) forecast is of utmost importance for heavy rainfall events leading to catastrophic floods, loss of life and property over the affected regions. These warnings could help the authorities to take necessary measures to reduce the damage to life and property. Also, accuracy of prediction of high risk events, i.e., the reliability of the forecast, is also a very important part of forecasting weather.

In the last couple of decades, several sophisticated numerical weather prediction (NWP) models have been developed around the world, for example Global Forecast System (GFS) at Environment Modeling Center (National Centers for Environmental Prediction [NCEP]), Unified Model (UM) at UKMet Office, Integrated Forecast system (IFS) at European Centre for Medium Range Weather Forecasting (ECMWF) and The Global Environmental Multiscale Model (GEM) at Environment Canada (Kalnay et al., 1990; Kanamitsu et al., 1991; Brown et al., 2012; IFS, 2012; Côté et al., 1998), which include many complex physical processes and advanced data assimilation schemes. In India, National Centre for Medium Range Weather Forecasting (NCMRWF) provides daily weather predictions based on two NWP models: T574 (Global Forecast System; GFS) and NCMRWF Unified Model (NCUM).

The upper Himalayan territories of Uttarakhand (Latitude 28.72°N to 31.45°N and Longitude 77.57°E to 81.03°E) are mainly covered with forests and mountains. These areas besides being important pilgrimage centers are also famous as tourist attractions especially during the hot summer months of the Indian subcontinent. During 14–17th June, 2013 Uttarakhand received heavy rainfall, and this when combined with the melting snow (due to high temperature during summer season) resulted in an aggravation of

* Corresponding author: Tel.: +91 1202403907; Mobile: +91 9999012055.
E-mail addresses: anumeha.dube@nic.in, anumeha@ncmrwf.gov.in, anumeha.dube@gmail.com (A. Dube).

http://dx.doi.org/10.1016/j.wace.2014.03.004

floods in this region (Kedarnath [30.73°N, 79.07°E] and adjoining areas). On 17th June alone, the state of Uttarakhand received more than 340 mm of rainfall (37 cm/day in Dehradun [30.32°N, 78.36°E]; as reported in the Climate Diagnostics Bulletin of India, June 2013 (Srivastava and Guhathakurta, 2013), which is 375% more than the daily normal (65.9 mm). The India Meteorological Department (IMD) reported a weekly departure of about 847% in the rainfall volume for the week ending on 19th June 2013 in Uttarakhand.

It has been consistently seen that NCUM shows better forecasting skills than T574 (Iyengar et al., 2010) (for an entire season) for wind, geopotential height, temperature and humidity at various levels. This is reflected in terms of relatively lower root mean square error (RMSE) and higher anomaly correlation. This is also reflected in forecast rainfall for an entire season as well as extreme cases. It is generally found that the improved skill in NCUM is reflected in the improved spatial organization of synoptic systems and associated rainfall which is missing in T574. This is largely attributed to the 4D-VAR data assimilation currently operational in NCUM as compared to GSI scheme operational in T574 which is based on the 3D-VAR data assimilation (Section 3).

The current study is based on the real time forecast obtained from NCUM and T574 and aims at comparing their performance in predicting the heavy rainfall event, of 17th and 18th June 2013, over Uttarakhand region. While we discuss briefly about the broad scale synoptic features that were observed during this time period, we do not go into the details of the causes and the physical processes leading to the event. Both the NWP models operational at NCMRWF provided a clear indication of 8–16 cm/day rainfall on 17th June, 2013 over Uttarakhand region up to 5 days (3 days) in advance in NCUM (T574). Although the location of the predicted highest rain was different in the two models, the forecasts (Day 1 through Day5 in NCUM and Day 1 through Day 3 in T574)

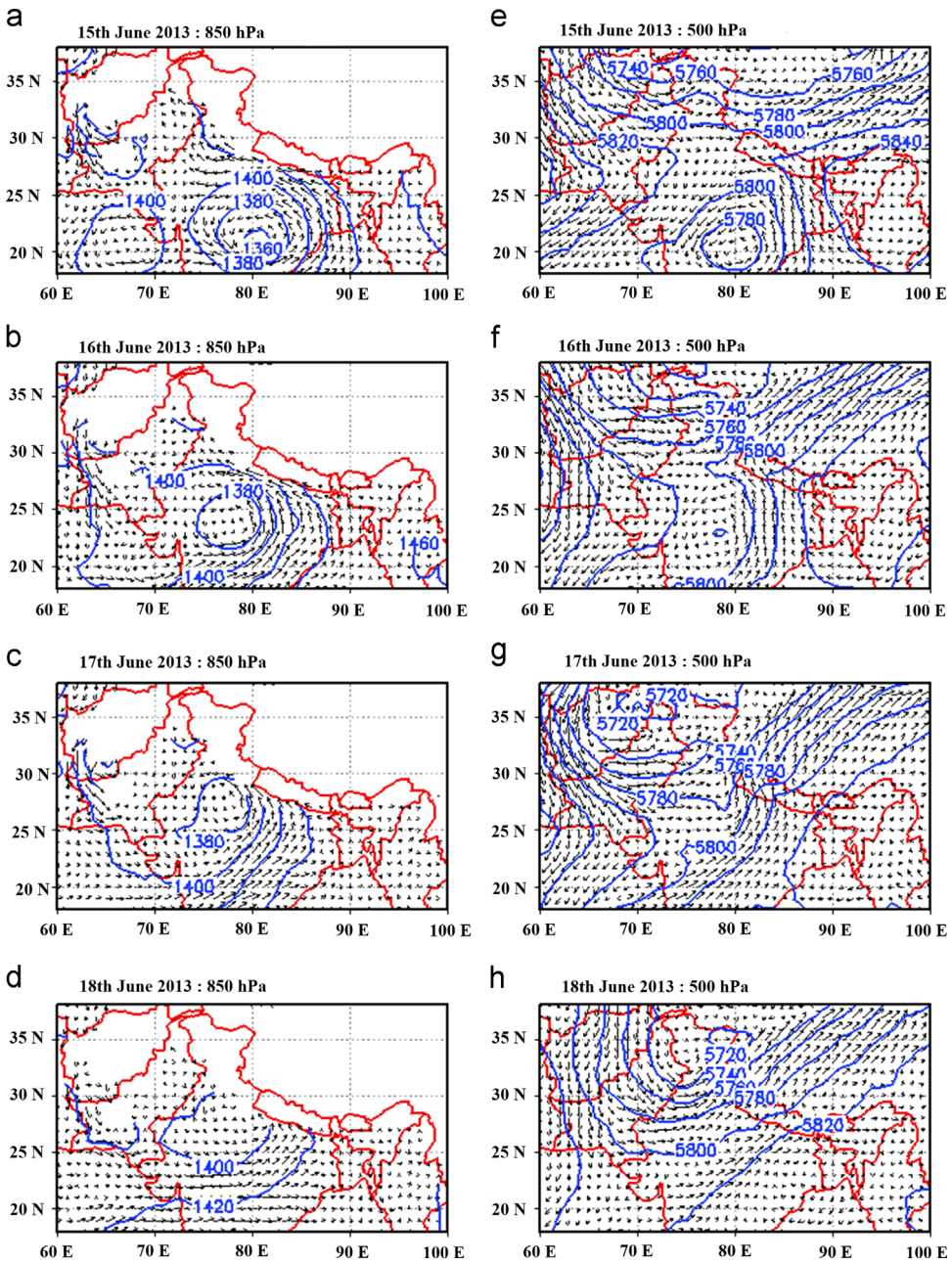

Fig. 1. 850 hPa (a–d) and 500 hPa (e–h) Wind Analysis (m/s) from NCUM for 15–18th June 2013.

consistently predicted high rainfall amounts over Uttarakhand and Himachal Pradesh.

In this study the CRA (Contiguous Rainfall Area) method is used for spatial verification of rainfall over Uttarakhand (Ebert and McBride, 1998, 2000). This method uses a pattern matching technique to determine the location error, as well as errors in area, mean and maximum intensity, and spatial pattern. The CRA technique is also used for event verification which calculates hit rates, false alarm rates, misses etc. by categorizing the forecasts for events themselves as hits, misses etc. Based on these a contingency table is constructed which is further used to calculate various verification statistics like Probability of Detection (POD), Equitable Threat Score (ETS) (Stanski et al., 1989), Hanssen and Kuipers Discriminant (HK) (Hanssen and Kuipers, 1965). Detailed explanation of the CRA verification technique is given in Section 4.

This manuscript is divided in the following sections: Section 2 deals with the observations, Section 2.1 describes the synoptic features that were observed during 17–18th June, 2013. This is followed by Section 2.2 which briefly describes the rainfall observations that are being used for verification in the current study. Section 3 touches upon the two deterministic models NCUM and T574 currently operational at NCMRWF, their main features and differences. Section 4 deals with the detailed description of the various verification methods used in this study as well as a description of the CRA verification technique. The results are discussed and explained in details in Section 5 based on both synoptic and CRA verification. Finally the important conclusions based on the entire study are summarized in Section 6.

2. Observations

2.1. Synoptic features as observed during 17–18 June 2013

Some major synoptic features observed on the 17th and 18th of June 2013 as described in the weather watch (17–18th of June morning, mid-day, evening and night) issued by the India Meteorological Department (IMD) (IMD 17-June-a, 2013; IMD 17-June-b, 2013; IMD 17-June-c, 2013; IMD 17-June-d, 2013; IMD 18-June-a, 2013; IMD 18-June-b, 2013; IMD 18-June-c, 2013 and IMD 18-June-d, 2013) are listed below:

- The axis of monsoon trough was passing through Bikaner (28.0167°N, 73.3119°E), Gwalior (26.22°N, 78.18°E), Gaya (24.75°N, 85.01°E) and Imphal (24.82°N, 93.95°E) and across the Gangetic West Bengal.
- A low pressure area which originated over northwest Bay of Bengal moved eastwards and was observed over Odisha (20.15°N, 85.5°E) on 13th June. It further intensified into a well marked low pressure area. The location of this system near the east coast of India on 15th June is clearly seen in Fig. 1(a), which shows the 850 hPa analyses wind from NCUM. Further northwestward movement of this low pressure system can be seen from the 850 hPa analysis wind for 16th to 18th June (Fig. 1(b–d)). This system sustained its northwestward movement till 18th June and weakened into a cyclonic circulation over Haryana (30.73°N, 76.78°E) and adjoining west Uttar Pradesh (26.85°N, 80.91°E).
- A western disturbance (WD) in the form of a trough in mid tropospheric level was observed around west Rajasthan (26.57°N, 73.84°E) on 16th June. This WD moved eastwards (towards east Rajasthan) and on 18th June it was observed near northern regions of India (Punjab [30.79°N, 76.78°E], Haryana, Uttarakhand and adjoining areas). This system finally moved away eastwards on 19th June 2013. The 500 hPa analysis wind from 15th to 18th June (Fig. 1(e–h)), shows the eastward movement of the WD in the form of a trough over north India.
- The analysis obtained from T574 is similar to that of NCUM and hence the figures are not displayed here.

2.2. Rainfall observations

Observed rainfall used for verification of the model forecasts is the IMD-NCMRWF merged satellite gauge (NMSG) data (Mitra et al., 2009, 2013). This rainfall data is a merged product of satellite estimates (Tropical Rainfall Measuring Mission [TRMM]) and

Table 1
T574 and NCUM model description and comparison.

	T574	NCUM
Horizontal Resolution	Spectral truncation of 574 waves in the zonal direction (T574) with a Gaussian grid of 1760 X 880 points. Approximately 23 Km resolution near equator).	N512 (~25 km at mid-latitudes) with a EW-NS grid of 1024x769 points.
Veritcal Levels	Hybrid sigma-pressure (64 levels). The hybrid coordinate system is terrain following in the lower levels and transforming to pure pressure levels in the upper levels.	70 Vertical Levels
Model Time Step	2 Minutes	10 minutes
Forecast Lead Time	10 Days	7 Days
Data Assimilation	Grid point Statistical Interpolation-GSI (Wu et al., 2002)	Four Dimensional Variational Data Assimilation System-4D VAR (Rawlins et al., 2007)
Dynamics	Spectral, Hybrid sigma-p, Reduced Gaussian grids	Non-hydrostatic dynamics with deep atmosphere. Height veritcal coordinates with levels transitioning from terrain following to height. Global Latitude Longitude Grids
Time Integration	Leapfrog/Semi-implicit	Semi-implicit time integration with 3D semi-Lagrangian advection

rain gauge observations (IMD) at 0.5° resolution, accumulated for 24 h daily at 03UTC. The forecast rainfall from T574 and NCUM are 24-hour accumulations valid at 03UTC to match with the observations.

3. NWP models at NCMRWF

In this section we briefly discuss about some noticeable differences between the formulations of the two models. Details about the deterministic models operational at NCMRWF can be found at (Rajagopal et al., 2007; Prasad et al., 2011) for T574 and (Rajagopal et al., 2012) for the Unified Model (NCUM). Table 1 gives a brief overview of the main features of the two models. The differences in the formulations of two models arise due to several factors including: horizontal and vertical resolutions, physical parameterizations, different time integration methods as well as data assimilation schemes etc. (Table 1). The most important among these are the different data assimilation schemes. T574 utilizes the Grid point Statistical Interpolation-GSI (Wu et al., 2002) which is based on the Three Dimensional Variational Data Assimilation System (3D-VAR) whereas NCUM uses Four Dimensional Variational Data Assimilation System (4D VAR) (Rawlins et al., 2007) scheme for data assimilation. 4D-Var is a simple generalization of 3D-Var and it takes into account the temporal evolution processes which lead to improved representation of synoptic systems in the initial conditions. Extensive studies have been conducted, at various meteorological organizations (UKMet Office, Meteorological Service of Canada, NCEP etc.), for comparing the respective skills of 4D-Var and 3D-Var in assimilating data and forming the initial conditions for different models. All these studies have helped in forming a consensus that the 4D-VAR performs better than the 3D-VAR scheme (Lorenc and Rawlins, 2005; Laroche et al., 2005). This is reflected in the better estimation of observed synoptic systems in the initial conditions (analysis) of the models using 4D-VAR for data assimilation. Additional details about the models' configuration and forecast products are summarized in Table 1.

		Intensity		
		Too Little	Approx. Correct	Too Much
Location	Close	Underestimated	Hit	Overestimated
	Far	Missed Event	Missed Location	False Alarm

Fig. 2. Structure of the event contingency table obtained from CRA verification.

4. Verification methods

Spatial verification of the rainfall forecasts in the present study is carried out using the CRA method. This method was developed for estimating the systematic errors in the rainfall forecasts (Ebert and McBride, 2000; Stefano and Marco, 2008 and Ebert and Gallus, 2009). It was one of the first methods to measure errors in predicted location and to separate the total error into components due to errors in location, volume and pattern. The steps involved in the CRA technique are described in (Ebert and McBride, 2000).

The CRA method is an object-oriented verification procedure suitable for gridded quantitative precipitation forecasts (QPFs). In the CRA framework a weather system is defined as a region bounded by a user specified isohyet (entity) of precipitation in the union of the forecast and observed rain field. This technique is then simply based on a pattern matching of two contiguous areas (entities), defined as the observed and forecast precipitation areas delimited by the chosen isohyet. The forecast and observed entities need not overlap, but they must be associated with each other, which means that they should be close to each other. The best match between the two entities can be determined either:

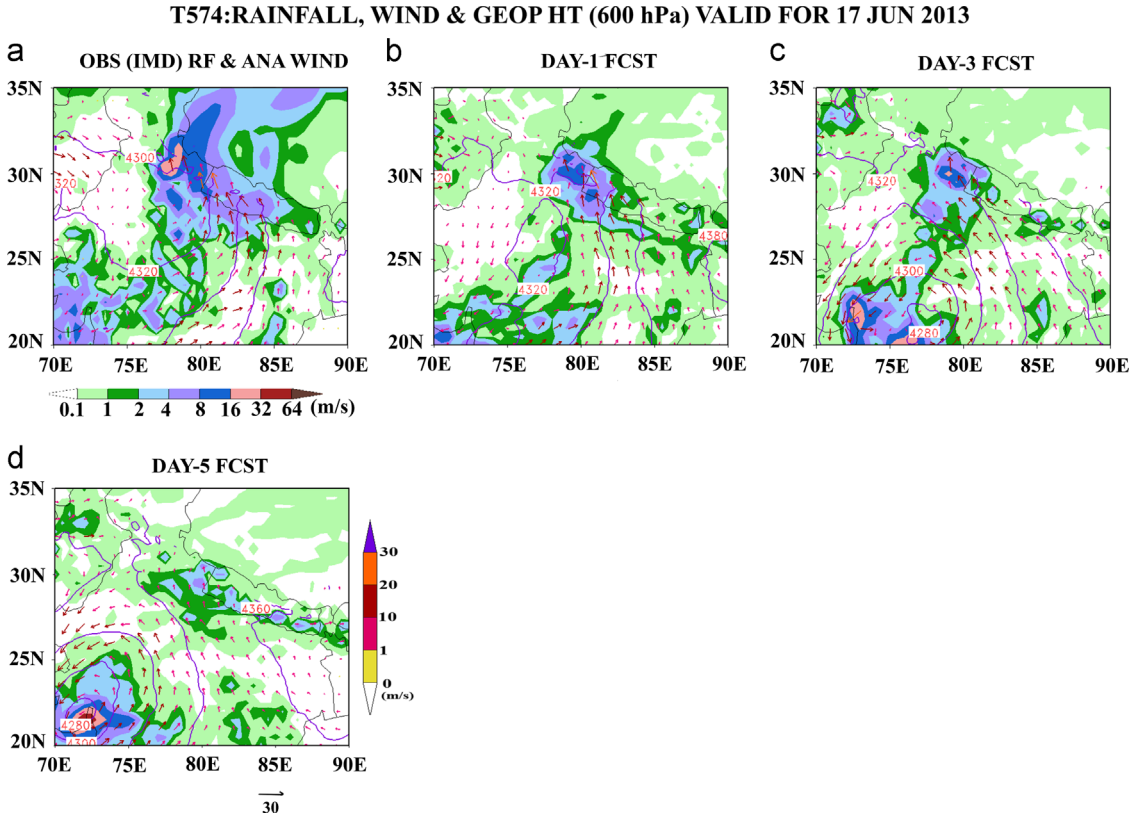

Fig. 3. Observed and T574 Model Predicted rainfall (cm/day), 650 hPa circulation (m/s) and geopotential height over Indian region valid for 03Z17June 2013.

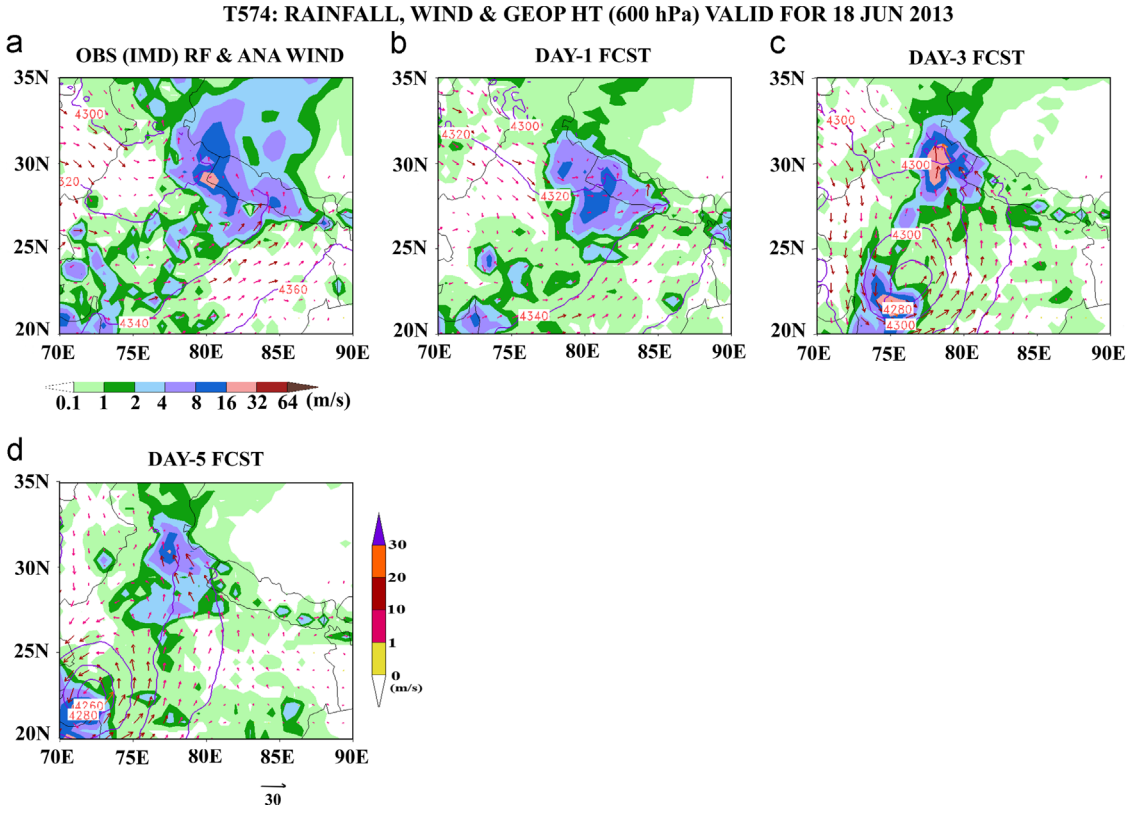

Fig. 4. Observed and T574 Model Predicted rainfall (cm/day), 650 hPa circulation (m/s) and geopotential height over Indian region valid for 03Z18June 2013.

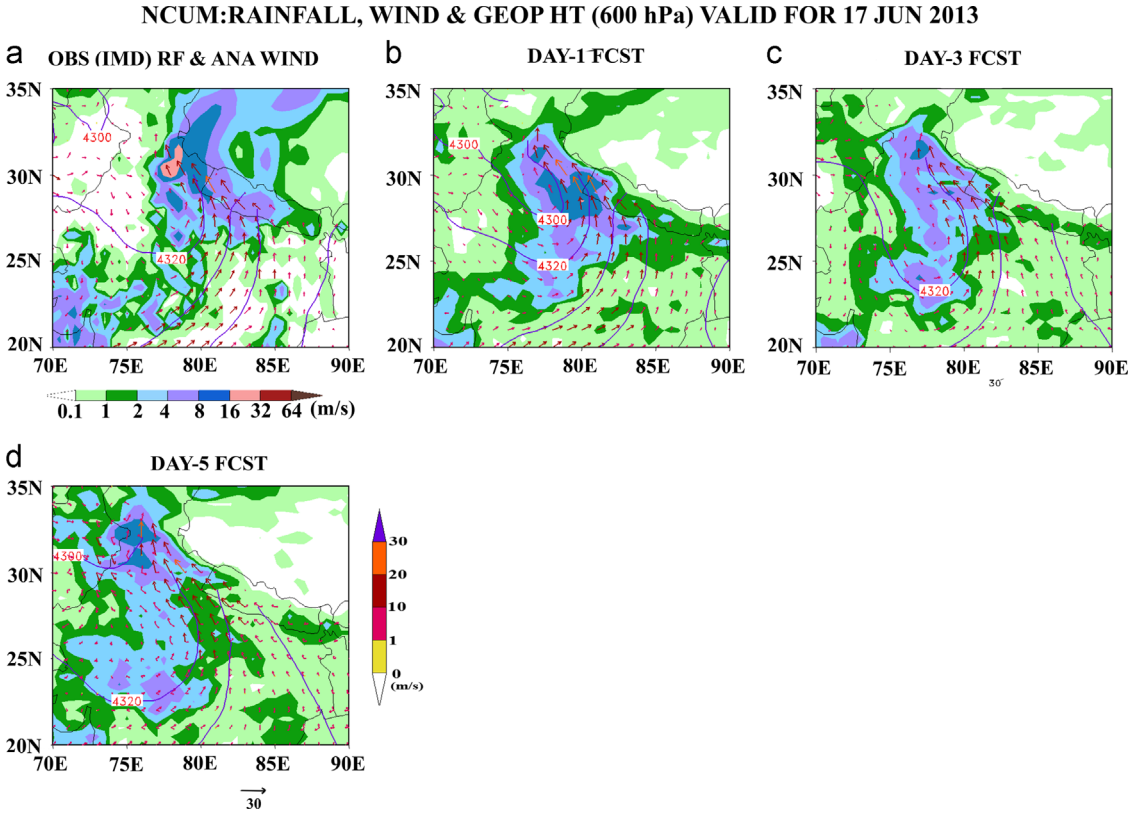

Fig. 5. Observed and NCUM Model Predicted rainfall (cm/day) and 600 hPa circulation (m/s) over Indian region valid for 03Z17June 2013.

(a) by maximizing the correlation coefficient, (b) by minimizing the total mean squared error, (c) by maximizing the overlap of the two entities, or (d) by overlaying the centers of gravity of the two entities. For a good forecast, all the methods should give very similar location errors. In the present study the best match is determined by maximizing the correlation.

For each entity that can be identified in forecast and observations, the CRA method determines the location, volume and pattern errors, which are then combined in the form of a total mean squared error (MSE). To estimate the location error, the forecast field is horizontally translated over the observed field until the best match is obtained. The location error is then simply the vector displacement of the forecast. MSE and its decomposition (location error, volume error and pattern error) are shown below:

$$MSE_{Total} = (F-O)^2 + (s_O - r s_F)^2 + (1-r^2)^2 s_F \quad (1)$$

where F (s_F) and O (s_O) are the mean (standard deviation) values of the forecast and observed precipitation respectively before obtaining the best match via shifting the forecast.

The spatial correlation between the original forecast and observed features (r) increases to an optimum value (r_{OPT}) in the process of correcting the location via pattern matching. The contribution to total error due to displacement, volume and pattern errors are estimated as

$$\left.\begin{aligned} MSE_{Displacement} &= 2 s_F s_O (r_{OPT} - r), \\ MSE_{Volume} &= (F^* - O^*), \text{ and} \\ MSE_{Pattern} &= 2 s_F s_O (1 - r_{OPT}) + (s_F - s_O)^2 \end{aligned}\right\} \quad (2)$$

where F^* and O^* are the mean values after shifting.

Displacement and pattern errors are associated with errors in dynamics (predicted flow) while volume error is associated with errors in physics (moisture) treatment. These components provide guidance for model developers when the statistics of error components are studied for large sample of cases.

In addition, the verified entities (forecasts in different rainfall thresholds) themselves may be classified as “hits”, “misses”, etc., according to how close the forecast location was to the observed location, and how well the maximum intensity was represented by the forecast. This event verification can be useful for monitoring forecast performance. Fig. 2 gives the structure of the event contingency table in the CRA verification procedure.

Based on this contingency table we can obtain information like number of hits (correct forecasts), misses (both location and event), false alarms, these can be used to verify a model’s performance in predicting rainfall in different thresholds. This

Table 2
Observed and forecast rainfall on 17th and 18th June. Observed station rainfall is recorded at Dehradun while the observed (NMSG) gridded and forecast rainfall amounts are the highest rainfall over the region of Uttarakhand (i.e., in a $2^\circ \times 2^\circ$ grid box encompassing Uttarakhand).

Date	Observed Rainfall (cm/day)		Forecast Rainfall (cm/day)					
			Day 1		Day 3		Day 5	
	Station (Dehradun)	Gridded (NMSG)	T574	NCUM	T574	NCUM	T574	NCUM
17-06-2013	37.0	24.9	12.9	14.7	20.3	10.5	6.8	15.3
18-06-2013	28.0	28.6	11.9	28.8	27.9	22.9	18.0	9.9

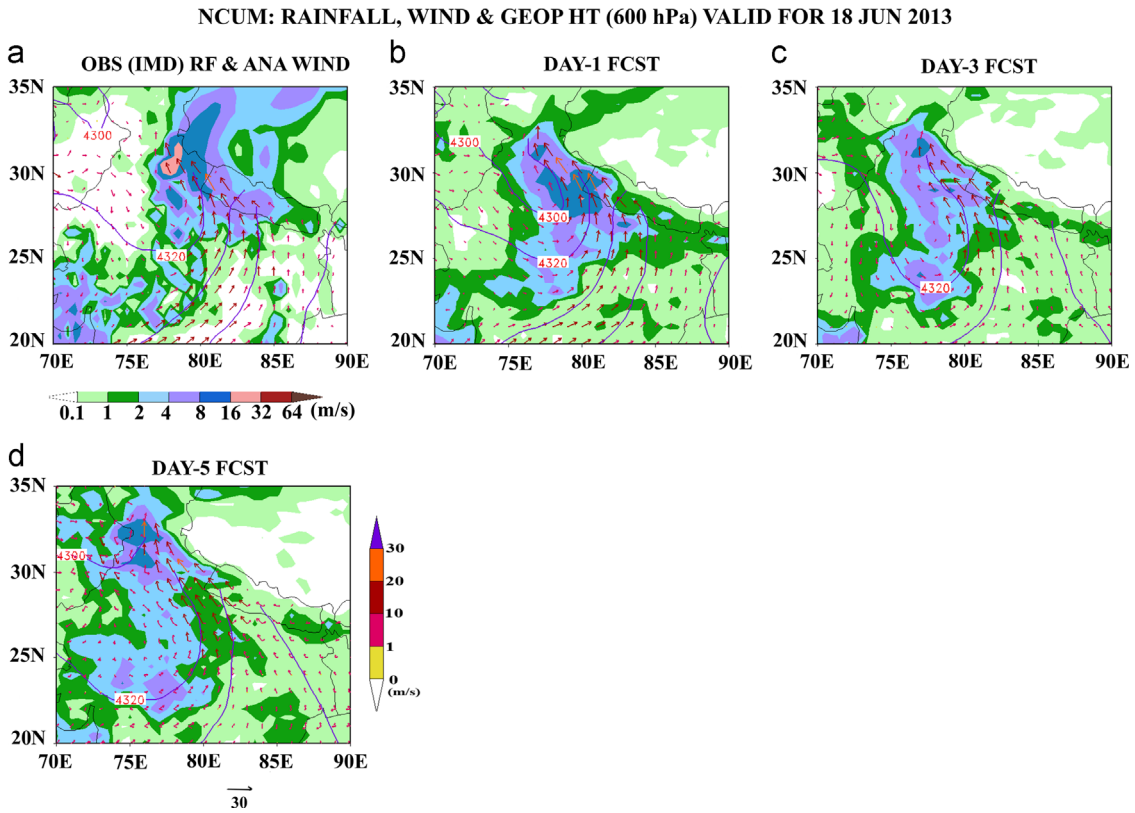

Fig. 6. Observed and NCUM Model Predicted rainfall (cm/day) and 600 hPa circulation (m/s) over Indian region valid for 03Z18June 2013.

contingency table can further be used to calculate verification statistics like POD, ETS and HK scores (Stefano and Marco, 2008).

In this study, the CRA method is used for verification of the rainfall forecast over Uttarakhand region. The verification is carried out over common grids of $0.5^\circ \times 0.5^\circ$ resolution. All grids over the neighboring seas and over Himalayas above 4000 m were masked out. We have obtained the contingency table defined above for the following rainfall ranges: 1–10 mm, 10–20 mm, 20–40 mm, 40–80 mm and 80–160 mm.

5. Results: verification of model forecasts

A qualitative summary of verification and intercomparison is presented first, mainly involving the synoptic features of the rainfall system. This is followed by a verification of quantitative precipitation forecast (QPF) (using the CRA technique) to quantify the forecast biases in the two models.

5.1. Synoptic features and rainfall

Figs. 4 and 5 show the observed and predicted rainfall along with circulation and geopotential height at 600 hPa over Uttarakhand region for T574 (approx. 3480 m AMSL (above mean sea level); location of flooding) valid on 17th and 18th of June 2013 respectively. Observed and model predicted peak rainfall amounts are also presented in Table 2. From Fig. 3 it can be seen that the Day 1 and Day 3 forecasts show moderate to high rainfall amounts over Uttarakhand and adjoining areas. Day 5 forecasts also show light rainfall over this region (the amount of rainfall is not as high as seen in Day 1 and Day 3 forecasts). However, the peak amount of observed precipitation (Table 2; Fig. 3(a)) is not captured by T574. Day 3 forecasts for 17th June show heavy rainfall (20 cm/day; Table 2) near the reported area of disaster. From Fig. 4 it can be seen that for 18th June, the model predicted very high amounts of rainfall (Table 2) in Uttarakhand only in the Day 3 forecast. However, this was absent in the Day 1 and Day 5 forecasts (Fig. 4(b, d)). The plots also show that there is some consensus between the observed and model predicted circulation patterns and geopotential height for Day 1 and Day 3 for 17th June whereas the comparison is poor beyond Day 1 in the case of forecast valid for 18th June. Beyond Day 1 the model is intensifying the inland low pressure system and its position is also much to the southwest of the observed location. These forecasts are dominated by the cyclonic circulation over Gujarat (23.2167°N, 72.6833°E) which is located in western India. This is clearly seen in Figs. 3(c, d) and 4(c, d).

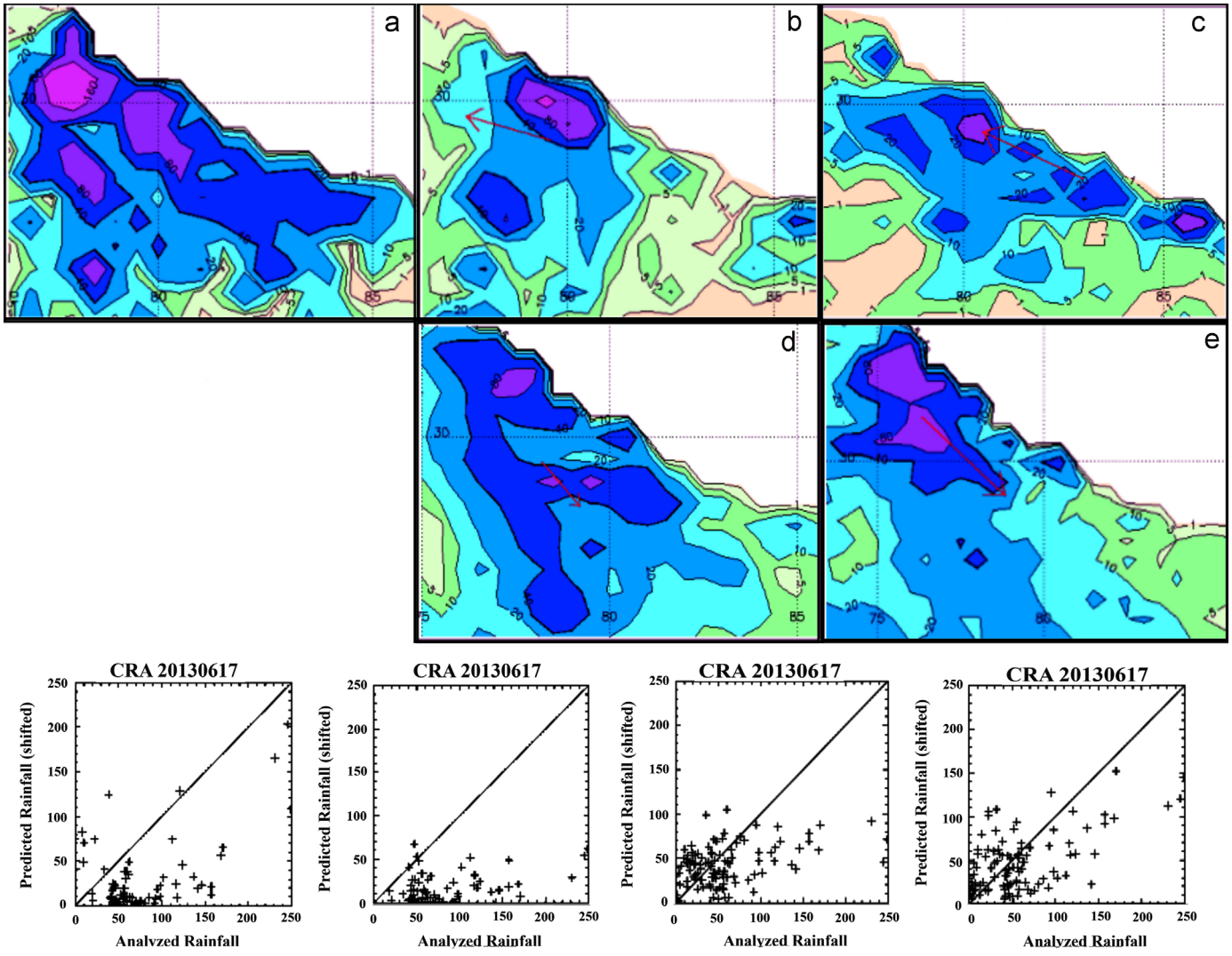

Fig. 7. Isohyets in mm for Uttarakhand region (a) Analysis (b) Day 3 and (c) Day 5 forecast from T574, (d) Day 3 and (e) Day 5 forecast from NCUM. Lower panel shows the number of matching grid points between T574 and NCUM from Day 3 and Day 5 forecasts valid on 17th June 2013.

A similar analysis is presented for NCUM (Figs. 5 and 6). Fig. 5 and Table 2 valid for 17th June show that the observed peak rainfall amounts are underestimated by approximately 50% in Day 1, Day 3 and Day 5 forecasts for 17th June. The rainfall pattern is also slightly displaced from its observed location in the Day 1, Day 3 and Day 5 forecasts. However, the model predicted rainfall for 18th of June shows that the amount of rainfall (Table 2) is nearly accurate for Day 1 and Day 3 forecasts (the observed peak rainfall amount is close to observation in Day 1 and underestimated by 20% in Day 3 forecast. Looking at the wind flow and geopotential height patterns from Figs. 5 and 6 we can see that the location of the low pressure system and intensity in the case of NCUM shows a better match with the analysis (Fig. 1(c–d, g–h)), as compared to T574, from Day 1 to Day 5 forecasts for both 17th and 18th of June.

5.2. CRA verification for rainfall on 17th and 18th June 2013

As a first step of CRA analysis (Section 4), entities based on rainfall rates were obtained, for this purpose experiments with different rainfall thresholds were performed. As an example: during the southwest monsoon season large parts of India regularly receive widespread rainfall in excess of 10 mm/day. Rainfall exceeding lower thresholds (1, 2 and 5 mm/day) spreads the CRA across large geographical areas, CRAs defined by higher thresholds of 10, 20, 40, 80 and 160 mm/day are used to isolate the events corresponding to a region and are associated with specific rain systems (offshore trough, monsoon trough, Bay of Bengal low pressure etc.).

As a next step, a pattern matching technique is used for estimating the location error (Section 3). In this case the best match between the forecast and observed entities is done by maximizing the correlation coefficient (Pearson correlation) between the forecast and observed fields. Figs. 7 and 8 show the CRA verification isohyets for Day 3 and Day 5 forecasts from T574 and NCUM valid for 17th and 18th of June respectively.

Tables 3 and 4 summarize the statistics obtained from CRA verification for Day 1 to Day 5 forecasts valid on the 17th and 18th June respectively. The mean square error comparison between the two models shows that NCUM has lesser error than T574 which implies that NCUM performs better than T574 in terms of matching the displacement, volume and pattern of the forecast precipitation entities. The tables also show the RMSE and Correlation Coefficient (CC) for the original and shifted rainfall (i.e., before and after the CRA procedure). The tabulated values of CC and RMSE are a direct indication of forecast

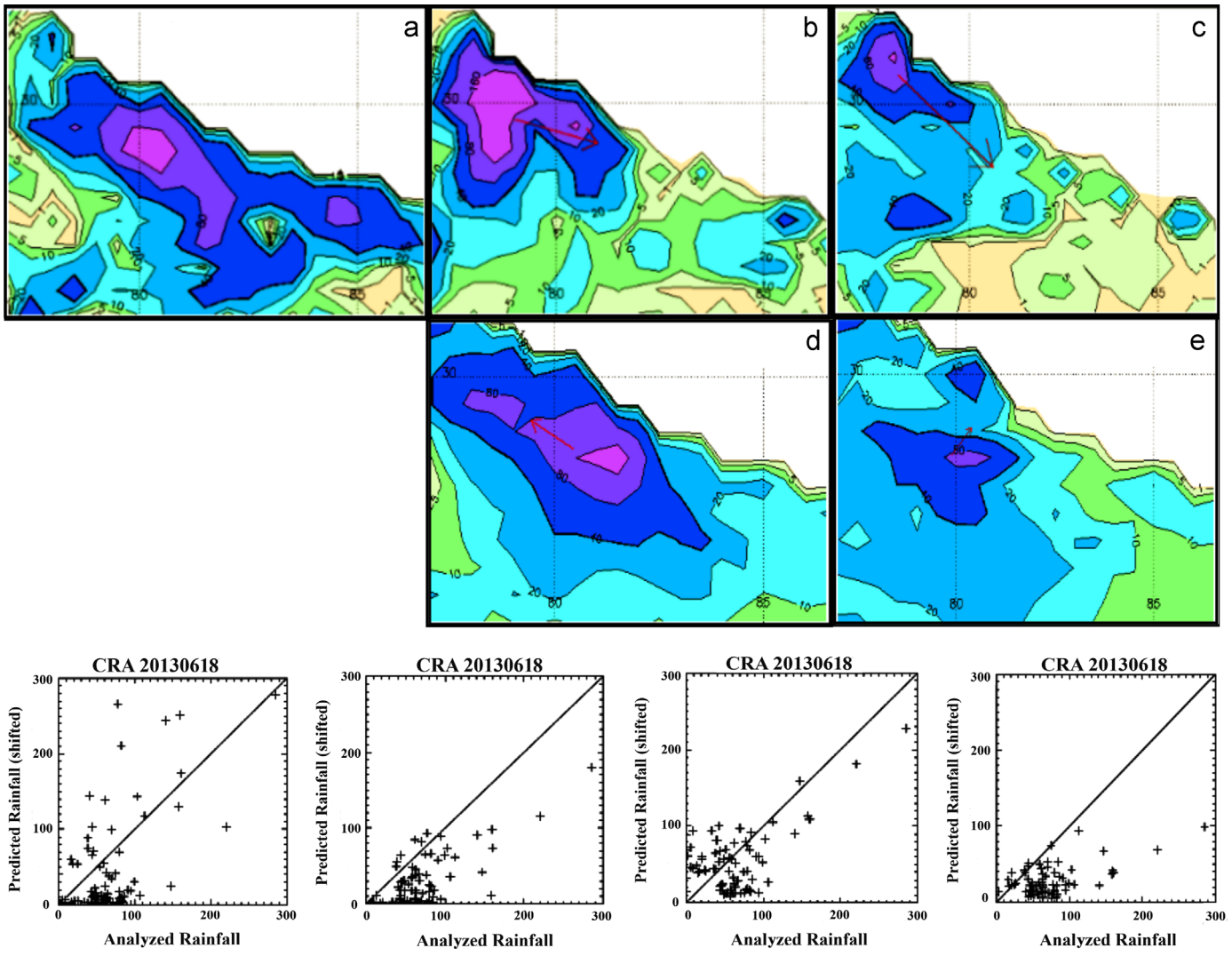

Fig. 8. Isohyets in mm for Uttarakhand region (a) Analysis (b) Day 3 and (c) Day 5 forecast from T574, (d) Day 3 and (e) Day 5 forecast from NCUM. Lower panel shows the number of matching grid points between T574 and NCUM from Day 3 and Day 5 forecasts valid on 18th June 2013.

accuracy. For forecasts with large errors improvement in CC from initial to shifted is large (Ebert and Gallus, 2009). On comparing the initial CC and RMSE we can see that NCUM (before the CRA procedure) has a higher CC and a lower RMSE which implies that it is a better forecast than T574. On comparing the relative change in the CC, after the shifting (during CRA verification), it can be observed that in T574 the change is much larger than NCUM (especially for 18th June forecast; Table 4) which once again confirms the better forecasting skill of NCUM (i.e., the forecast entities in T574 need to be shifted more to obtain a better CC as compared to NCUM).

Table 3
MSE, initial and shifted RMSE and correlation coefficient for Day 1 to Day 5 forecasts obtained from the CRA verification for rainfall forecast from NCUM and T574 valid on 17th June 2013.

Date	Mean square error		Initial correlation		Shifted correlation		Initial RMSE		Shifted RMSE	
	NCUM	T574	NCUM	T574	NCUM	T574	NCUM	T574	NCUM	T574
2013061724	2939.98	5115.45	0.23	0.06	0.45	0.44	54.22	71.52	46.21	60.48
2013061748	2339.06	6142.94	0.24	−0.15	0.41	0.56	48.36	78.38	46.42	60.80
2013061772	3088.20	5244.44	0.05	0.24	0.42	0.47	55.57	72.42	47.59	64.81
2013061796	3649.98	6878.32	0.03	−0.01	0.41	0.54	60.42	82.94	56.76	74.12
20130617120	5046.61	7136.40	−0.35	−0.16	0.61	0.38	71.04	84.48	41.73	78.44

Table 4
MSE, initial and shifted RMSE and correlation coefficient for Day 1 to Day 5 forecasts obtained from the CRA verification for rainfall forecast from NCUM and T574 valid on 18th June, 2013.

Date	Mean square error		Initial correlation		Shifted correlation		Initial RMSE		Shifted RMSE	
	NCUM	T574	NCUM	T574	NCUM	T574	NCUM	T574	NCUM	T574
2013061824	3209.68	2337.36	0.28	0.27	0.70	0.36	56.65	48.35	37.87	52.22
2013061848	2672.02	3492.35	0.30	0.33	0.60	0.43	51.69	59.10	43.20	54.50
2013061872	2135.72	7223.51	0.45	−0.02	0.56	0.57	46.21	84.99	42.25	58.61
2013061896	2714.22	5499.39	0.45	−0.08	0.66	0.49	52.10	74.16	42.12	59.85
20130618120	4476.41	5630.67	0.45	−0.25	0.53	0.70	66.91	75.04	58.25	50.99

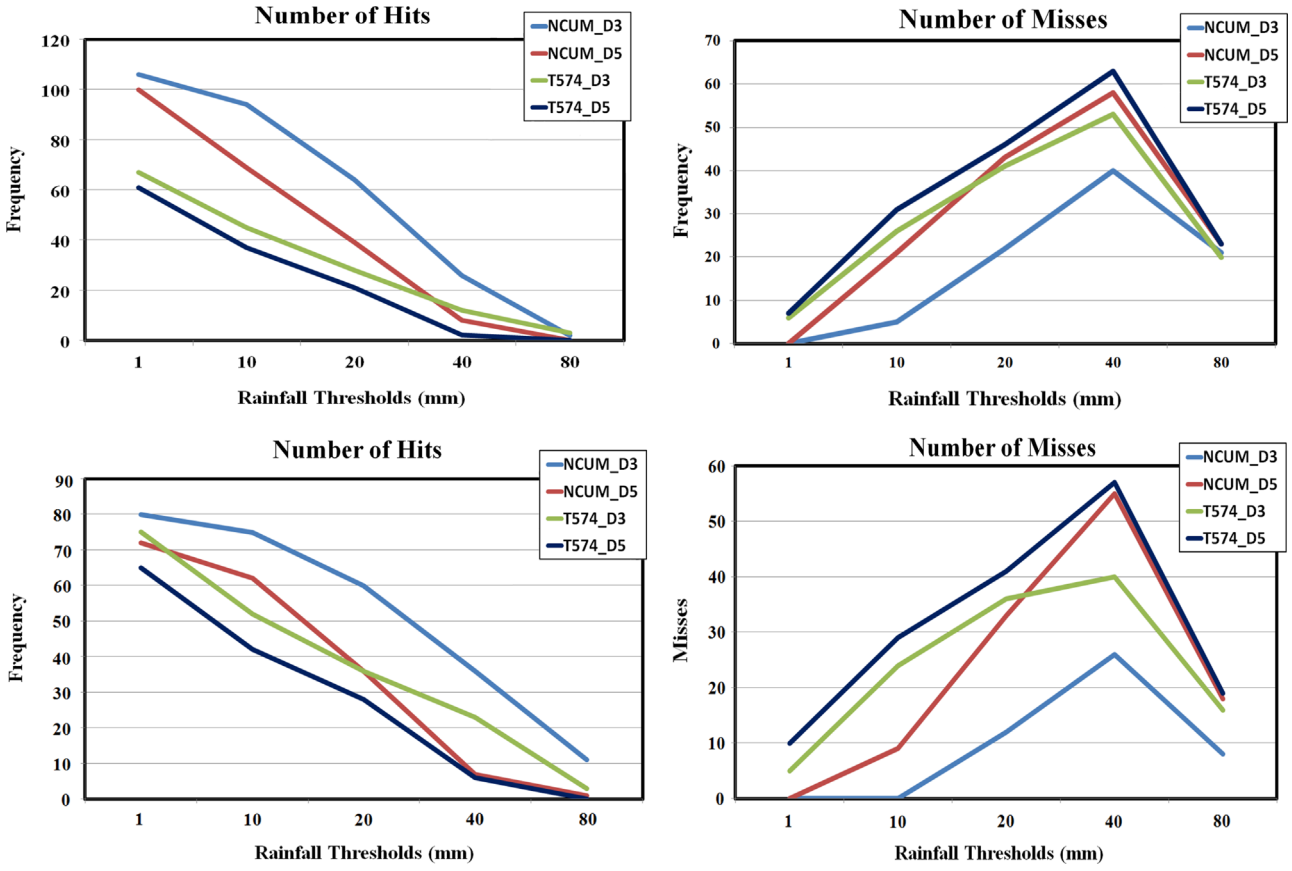

Fig. 9. Number of hits and misses based on the event verification during CRA procedure. Panels (a) and (b) correspond to number of hits and misses for Day 3 and Day 5 forecasts valid on 17th June and panels (c) and (d) correspond to the hits and misses for Day 3 and Day 5 forecasts valid on 18th June. These are based on ≤1 mm/day, 1–10 mm/day, 10–20 mm/day, 20–40 mm/day, 40–80 mm/day rainfall thresholds.

5.3. Event verification: verification of QPF statistics

Another way that CRA technique can quantify visual verification is to categorize the forecasts for the events themselves as "hits", "misses", etc., depending on whether their location and intensity were well predicted.

In the current case we have calculated the CRA statistics for a number of rainfall thresholds ranging from 10 mm/day to 160 mm/day. Based on these the numbers of hits, misses, false alarms etc., were calculated during the CRA analysis. Fig. 9(a–d) shows the frequency of hits and misses for 17th and 18th June respectively for different rainfall thresholds ($\leq$1 mm/day, 1–10 mm/day, 10–20 mm/day, 20–40 mm/day and 40–80 mm/day). It is very clearly seen from these figures that NCUM has a higher frequency of hits and a lower frequency of misses as compared to T574 for all the rainfall thresholds.

Figs. 10 and 11 show the POD, ETS and HK score in the form of bar graphs for Day 1 to Day 5 forecasts of T574 and NCUM valid for 17th and 18th June respectively. These statistics were calculated for two different rainfall thresholds (10–20 mm; left panels and 20–40 mm; right panels) for both the models. These statistics were calculated based on a contingency table, which contains the number of hits, misses and false alarms (Fig. 2; Section 3).

POD is defined as the fraction of observed events that were also correctly forecasted; therefore a high POD indicates good forecast skill of a model. In the current case a high POD would imply that many forecast entities with intensities approximately matching the observations were lying close enough to the observed entities

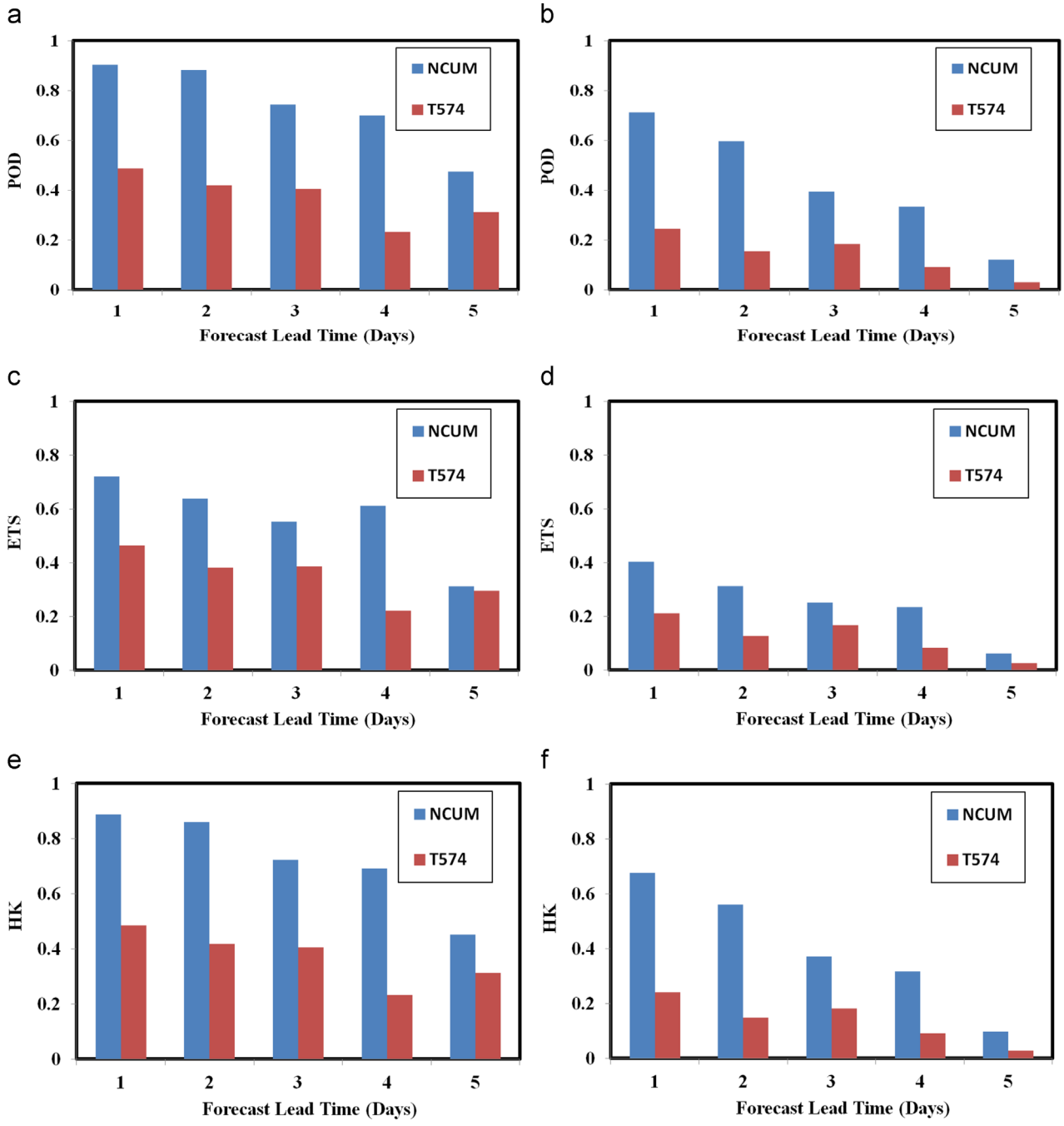

Fig. 10. Bar graphs showing the various statistics for T574 and NCUM for Day 1 to Day 5 forecasts valid for 17th June 2013 based on 10–20 mm/day (a, c and e) and 20–40 mm/day (b, d and f) rainfall thresholds.

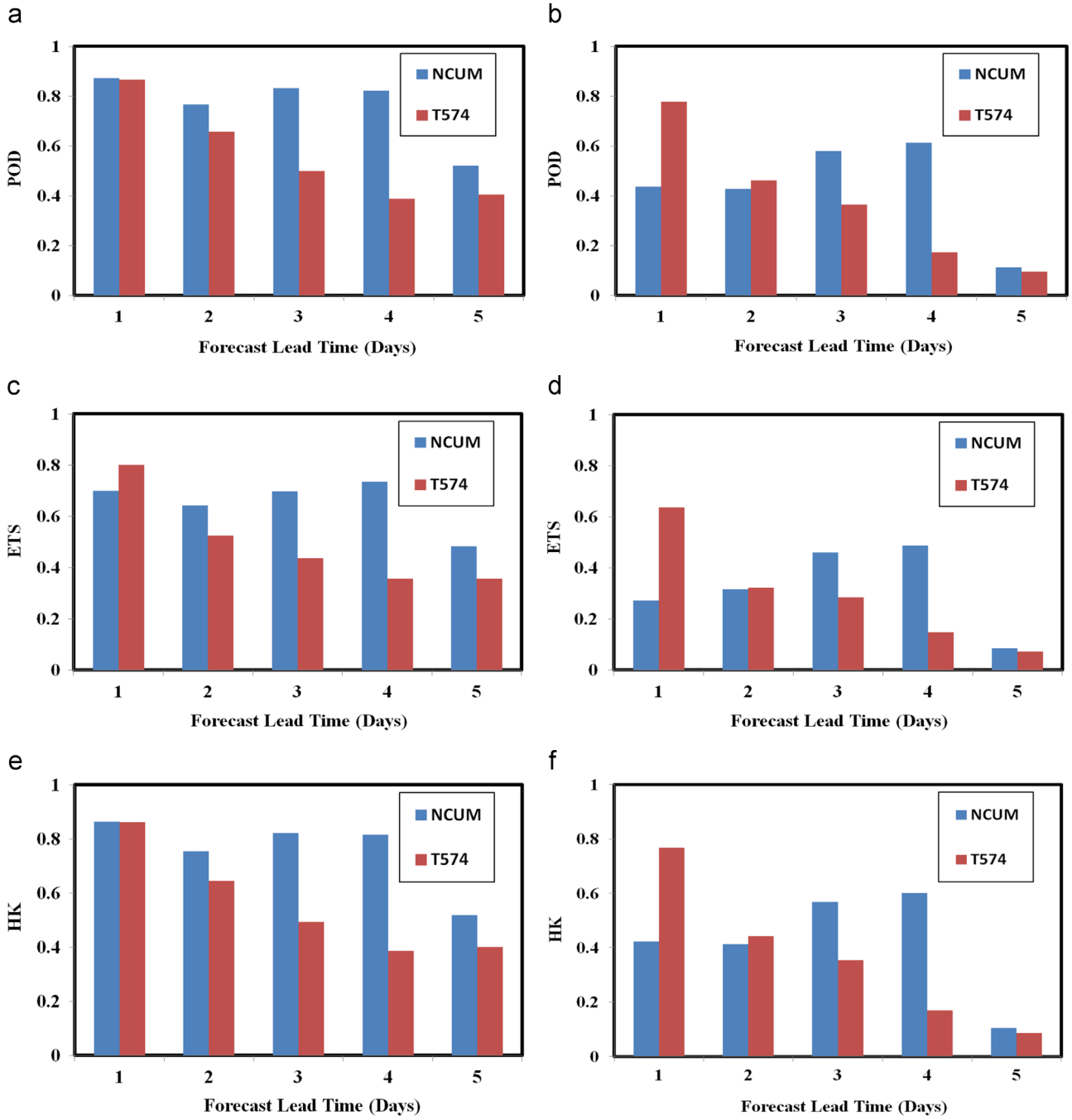

Fig. 11. Bar graphs showing the various statistics for T574 and NCUM for Day 1 to Day 5 forecasts valid for 18th June 2013 based on 10–20 mm/day (a, c and e) and 20–40 mm/day (b, d and f) rainfall thresholds.

hence having a higher number of hits (Fig. 9). From the two Figs. 10 and 11, it is seen that POD is consistently higher for NCUM (Day 1 to Day 5) for the forecast valid on 17th. For the forecast valid on 18th of June, for 10–20 mm rainfall threshold NCUM consistently shows a higher POD than T574 as in the previous case. On the other hand, for 20–40 mm rainfall threshold T574 shows a higher POD for Day 1 and Day 2 forecasts as compared to NCUM. For Day 3 to Day 5 forecasts, in the same rainfall threshold, NCUM once again shows a higher POD than T574.

Threat Score (TS or Critical Success Index [CSI]) measures the fraction of observed and/or forecast events that were correctly predicted. It can be thought of as the accuracy when correct negatives have been removed from consideration, i.e., TS is only concerned with forecasts that count. TS depends on climatological frequency of events (poorer scores for rarer events) since some hits can occur purely due to random chance. Therefore, ETS was designed to help offset this tendency. ETS measures the fraction of events that are correctly predicted accounting for hits by random chance. In present scenario a high ETS would imply that there is a large number of correctly predicted forecast entities near to the location of the matching observed entities (hits) and lesser number of forecast entities far away from the observations (misses and false alarms). For 17th June ETS is higher for Day 1 to Day 5 forecasts obtained from NCUM. For the Day 1 and Day 2 forecasts valid on 18th June, ETS in T574 is higher for both the rainfall thresholds. However, for Day 3 to Day 5 NCUM shows a higher ETS as compared to T574 for both the rainfall thresholds. Also ETS decreases with increasing forecast lead time for both the models.

HK score, also known as the True Skill Score (TSS), is defined as the difference between the hit rate and the false alarm rate (Hanssen and Kuipers, 1965). A high HK score indicates more hits relative to false alarms. The this study a higher HK score implies that the number of hits i.e., the number of forecast entities which were predicted with intensity and location close to the observed entities is higher as compared to the false alarms which is defined as a forecast entity which has intensity much higher than the observations and its predicted location is far away. In this case NCUM shows a higher HK score for the forecast valid on 17th June. The HK score for NCUM is much closer to 1 (a perfect score) for Day 1 and Day 2 forecasts and decreases after this for 10–20 mm rainfall threshold. However, for 20–40 mm rainfall threshold the score values are lower for both the models. For Day 1 forecast valid on 18th June, T574 shows a higher HK score than NCUM, but from Day 2 to Day 5 forecasts NCUM shows better skills than T574.

6. Conclusions

In this paper a comparison of the relative skills of T574 and NCUM in predicting the extreme rainfall (and the associated synoptic systems) observed over Uttarakhand and adjoining areas during 17th and 18th of June 2013 is carried out. This rainfall was a result of many factors including the interaction of two synoptic systems: a WD (observed from 16th to 18th June) in upper levels and a low pressure system in the lower levels which originated in the Bay of Bengal on the 13th of June and moved north westwards till 18th June 2013. The intensity of rainfall in this case was compounded due to the complex orography of the region and the prevalent summer time conditions, hence making it a rare extreme event and a challenge for weather forecasters.

NCUM forecasts successfully capture all aspects of the synoptic setting resulting in an improved prediction of location and amount of rainfall observed in the affected area. While the location and movement of the WD was accurately predicted by both the models, the direction of movement of low pressure system was correctly predicted only in NCUM (even in Day 5 forecasts). This efficiency of NCUM in predicting the low pressure system and its north-westerly movement resulted in a better estimation of the resulting rainfall (location and amount) as compared to T574 in the analysis area.

The spatial verification of model predicted rainfall is used here for the first time for such a rare extreme event. T574 largely underestimates the average rain rate and the rain volume as compared to NCUM which shows lower percentage errors and total mean square error and RMSE and better correlation coefficient. Event verification by making use of a contingency table shows that NCUM has higher number of hits and lower misses than T574. A comparison based on statistical verification scores like POD, ETS and HK reaffirms the better performance of NCUM.

Using ensemble forecasting for weather prediction can prove to be very useful in catching an extreme/rare event. Global Ensemble Forecast System (GEFS) is an ensemble prediction system that is running operationally at NCMRWF. An important extension of our work is the verification of the ensemble products which is under progress.

Acknowledgments

The authors are thankful for valuable input and suggestions from Scientists at NCMRWF.

The authors are grateful to Dr Elizabeth Ebert, CAWCR, Melbourne, Australia for providing the spatial verification package. Authors also acknowledge the comments and suggestions by anonymous reviewers.

References

Brown, A., Milton, S., Cullen, M., Golding, B., Mitchell, J., Shelly, A., 2012. Unified modeling and prediction of weather and climate: a 25-year journey. Bull. Am. Meteor. Soc. 93, 1865–1877.

Côté, J., Gravel, S., Méthot, A., Patoine, A., Roch, M., Staniforth, A., 1998. The operational CMC–MRB global environmental multiscale (GEM) model. Part I: design considerations and formulation. Mon. Weather Rev. 126, 1373–1395.

Disaster Update, 18-June, 2013. National Institute of Disaster Management (NIDM). ⟨http://nidm.gov.in/PDF/DU/2013/June/18-06-13.pdf⟩.

Disaster Update, 19-June, 2013. National Institute of Disaster Management (NIDM). ⟨http://nidm.gov.in/PDF/DU/2013/June/19-06-13.pdf⟩.

Ebert, E.E. and McBride J.L., 1998. Routine verification of NWP quantitative precipitation forecasts for weather systems, In: 12th Conference on Numerical Weather Prediction, Phoenix, AZ. American Meteorological Society, pp. J119–J122.

Ebert, E.E., McBride, J.L., 2000. Verification of precipitation in weather systems: Determination of systematic errors. J. Hydrol. 239, 179–202.

Ebert, E.E., Gallus, W.A., 2009. Toward better understanding of the contiguous rain area (CRA) verification method for spatial verification. Weather Forecast. 24, 1401–1415.

Hanssen A.J. and Kuipers, W.J., 1965. On the relationship between the frequency of rain and various meteorological parameters. Koninklijk Neferlands Meteorologist Institua Meded. Verhand, 81, pp. 2-25.

IFS Documentaion – Cy38r1, 2012. Full Scientific and Technical Documentation of the Integrated Forecast System. ⟨http://www.ecmwf.int/research/ifsdocs⟩.

IMD, 17-June-a, 2013. All India Weather Bulletin (Morning). India Meteorological Department (IMD), Ministtry of Earth Sciences, Earth System Science Organisation, Government of India. (⟨http://www.imd.gov.in/section/nhac/forecast_7days/archive/ai17062013mor.pdf⟩).

IMD, 17-June-b, 2013. All India Weather Bulletin (Mid Day). India Meteorological Department (IMD), Ministry of Earth Sciences, Earth System Science Organisation, Government of India. (⟨http://www.imd.gov.in/section/nhac/forecast_7days/archive/ai17062013mid.pdf⟩).

IMD, 17-June-c, 2013. All India Weather Bulletin (evening). India Meteorological Department (IMD), Ministry of Earth Sciences, Earth System Science Organisation, Government of India. (⟨http://www.imd.gov.in/section/nhac/forecast_7days/archive/ai17062013eve.pdf⟩).

IMD, 17-June-d, 2013. All India Weather Bulletin (Night). India Meteorological Department (IMD), Ministry of Earth Sciences, Earth System Science Organisation, Government of India. (⟨http://www.imd.gov.in/section/nhac/forecast_7days/archive/ai17062013nig.pdf⟩).

IMD, 18-June-a, 2013. All India Weather Bulletin (Morning). India Meteorological Department (IMD), Ministry of Earth Sciences, Earth System Science Organisation, Government of India. (⟨http://www.imd.gov.in/section/nhac/forecast_7days/archive/ai18062013mor.pdf⟩).

IMD, 18-June-b, 2013. All India Weather Bulletin (Mid Day). India Meteorological Department (IMD), Ministry of Earth Sciences, Earth System Science Organisation, Government of India. (⟨http://www.imd.gov.in/section/nhac/forecast_7days/archive/ai18062013mid.pdf⟩).

IMD, 18-June-c, 2013. All India Weather Bulletin (Evening). India Meteorological Department (IMD), Ministry of Earth Sciences, Earth System Science Organisation, Government of India. (⟨http://www.imd.gov.in/section/nhac/forecast_7days/archive/ai187062013eve.pdf⟩).

IMD, 18-June-d, 2013. All India Weather Bulletin (Night). India Meteorological Department (IMD), Ministry of Earth Sciences, Earth System Science Organisation, Government of India. (⟨http://www.imd.gov.in/section/nhac/forecast_7days/archive/ai18062013nig.pdf⟩).

Iyengar, G.R., Ashrit, R., Das Gupta, M., Chourasia, M., Sharma, K., Prasad, V.S., Rajagopal, E.N., Mitra, A.K., Mohandas, S., Harenduprakash, L., 2010. NCMRWF & UKMO global model forecast verification: monsoon 2010. NCMRWF Internal Report, 43–48.

Kalnay, E., Kanamitsu, M., Baker, W.E., 1990. Global Numerical weatherw prediction at the national meteorological center. Bull. Am. Meteor. Soc. 71, 1410–1428.

Kanamitsu, M., Alpert, J.C., Campana, K.A., Caplan, P.M., Deaven, M., Iredell, B., Katz, H., Pan, L., Selaand, J., White, G.H., 1991. Recent Changes Implemented into the Global Forecast System at NMC. Weather Forecast. 6, 425–435.

Laroche, S., and Gauthier, P., Tanguay, M., Pellerin, S., Morneau, J., Koclas, P., Ek, N., 2005. Evaluation of the operational 4D-Var at the Meteorological Service of Canada. In: Proceedings of the Fourth WMO International Symposium on Assimilation of Observations in Meteorology and Oceanography, Prague, Czech Republic, World Meteorological Organization. p. 139.

Lorenc, A.C., Rawlins, F., 2005. Why does 4D-Var beat 3D-Var? Q. J. R. Meteorol. Soc. 131, 3247–3257.

Mitra, A.K., Bohra, A.K., Rajeevan, M.N., Krishnamurti, T.N., 2009. Daily Indian precipitation analysis formed from a merge of rain-gauge data with the TRMM TMPA satellite-derived rainfall estimates. J. Meteorol. Soc. Jpn. 87 (A), 265–279.

Mitra, A.K., Momin, I.M., Rajagopal, E.N., Basu, S., Rajeevan, M.N., Krishnamurti, T.N., 2013. Gridded daily indian monsoon rainfall for 14 seasons: merged TRMM and IMD gauge analyzed values. J. Earth Syst. Sci. 122 (5), 1173–1182.

Prasad, V.S., Mohandas, S., Das Gupta, M., Rajagopal, E.N., Dutta, S.K., 2011. Implementation of upgraded Global Forecasting Systems (T382L64 and T574L64) at NCMRWF, NCMRWF Technical Report, pp. 1–72.

Rajagopal, E.N., Das Gupta, M., Mohandas, S., Prasad, V.S., George, John P., Iyengar, G.R., Kumar, D., Preveen, 2007. Implementation of T254L64 Global Forecast System at NCMRWF, NCMRWF Technical Report, pp. 1–42.

Rajagopal, E.N., G.R. Iyengar, G.R., George, John P., Das Gupta, M., Mohandas, S., Siddharth, R., Gupta, A., Chourasia, M., Prasad, V.S., Aditi, Sharma, K., Amit Ashish, 2012. Implementation of Unified Model based Analysis-Forecast System at NCMRWF, NMRF/TR/2/2012, 45 p.

Rawlins, F., Ballard, S., Bovis, K., Clayton, A., Li, D., Inverarity, G., Lorenc, A.C., Payne, T., 2007. The met office global four-dimensional variational data assimilation scheme. Q. J. R. Meteorol. Soc. 133, 347–362.

Southwest monsoon-June, 2013. Daily Flood Situation Report. Summary of Important Events as on 17-06-2013. Ministry of Home Affairs (Disaster Management Division), SITREP NO-17/2013, No.32-20/2013-NDM-I. ⟨http://www.ndmindia.nic.in/flood-2013/floodsJune-2013.htm⟩.

Southwest monsoon-July, 2013. Daily Flood Situation Report. Summary of Important Events as on 17-06-2013. Ministry of Home Affairs (Disaster Management Division), SITREP NO-19/2013, No. 32-20/2013-NDM-I. ⟨http://www.ndmindia.nic.in/flood-2013/floodsJuly-2013.htm⟩.

Srivastava, A.K., Guhathakurta, P., 2013. Climate Diagnostics Bulletin of India June 2013, Near Real-Time Analysis. Issue number 208. India Meteorological Department, Ministry of Earth Sciences, Earth System Science Organisation, Government of India. ⟨www.imdpune.gov.in/research/ncc/climatebulletin/cdbi_Jun_2013.pdf⟩.

Stanski, H.R., Wilson, L.J., Burrows, W.R., 1989. Survey of common verification methods in meteorology, World Weather Watch Technical Report No.8.

Stefano, M., Marco, C., 2008. Forecast Verification: a summary of common approaches and examples of application, FORALPS Technical Report 5. Università degli Studi di Trento, Dipartimento di Ingegneria Civile e Ambientale, Trento, Italy (60 pp.).

Wu, W.S., Purser, R.J., Parrish, D.F., 2002. Three-dimensional variational analysis with spatially inhomogeneous covariances. Mon. Weather Rev. 130, 2905–2916.